

Supporting Information

Acyclic Cucurbit[*n*]uril-Based Nanosponges Significantly Enhance the Photodynamic Therapeutic Efficacy of Temoporfin *in Vitro* and

In Vivo

Zizhen Zhao,^a Jingyu Yang,^a Yamin Liu,^c Shuyi Wang,^{a,b} Wei Zhou,^a
Zhan-Ting Li,^a Dan-Wei Zhang,^a Da Ma^{*b}

^aDepartment of Chemistry, Fudan University, 220 Handan Road, Shanghai, 200433, China.

^bSchool of Pharmaceutical Engineering & Institute for Advanced Studies, Taizhou University, 1139 Shifu Road, Taizhou, Zhejiang 318000, China.

^cFrontiers Science Center for Transformative Molecules, School of Chemistry and Chemical Engineering, National Center for Translational Medicine, Shanghai Jiao Tong University, Shanghai, 200240, China

Table of Contents

| | |
|--------------------------------|----|
| 1. Synthetic Procedure | S2 |
| 2. Characterization | S3 |
| 3. Host-Guest Chemistry | S5 |
| 4. <i>In vitro</i> Study | S7 |
| 5. <i>In Vivo</i> Study | S9 |

Synthetic Procedures

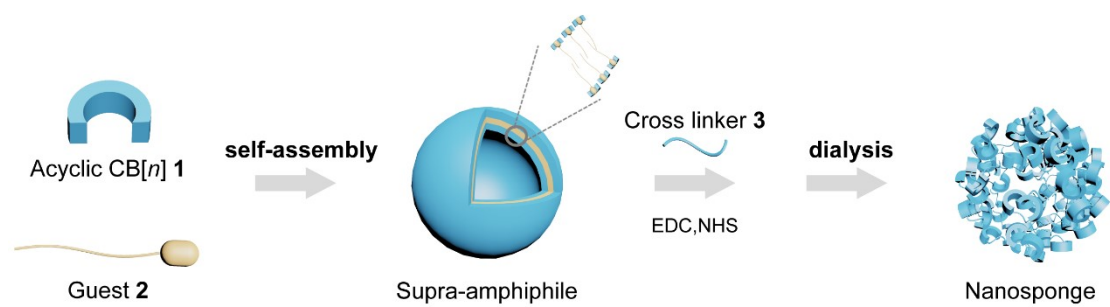


Fig. S1. Synthetic procedures of nanosponges.

Characterization

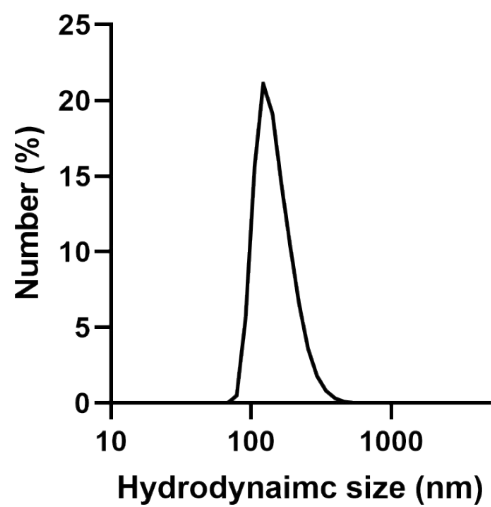


Fig. S2. DLS profile of the supra-amphiphiles with an average hydrodynamic size of 152 nm.

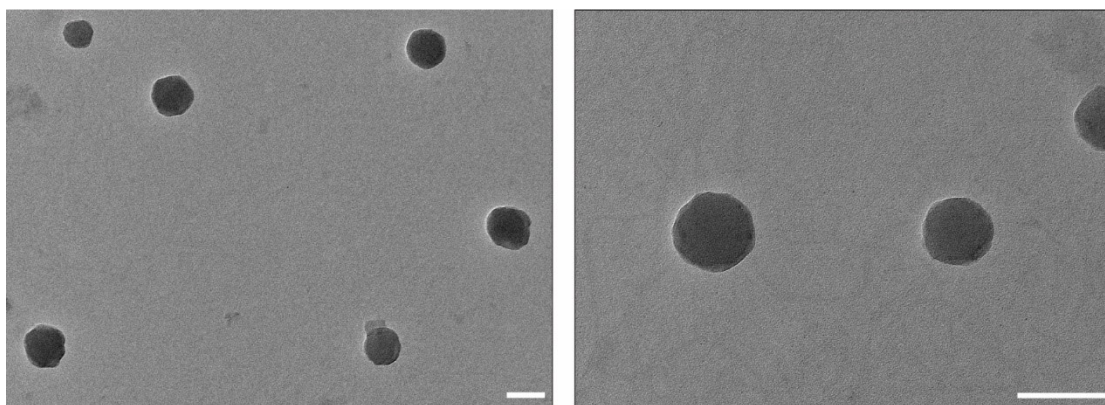


Fig. S3. TEM image of nanosponges. Scale bar: 100 nm.

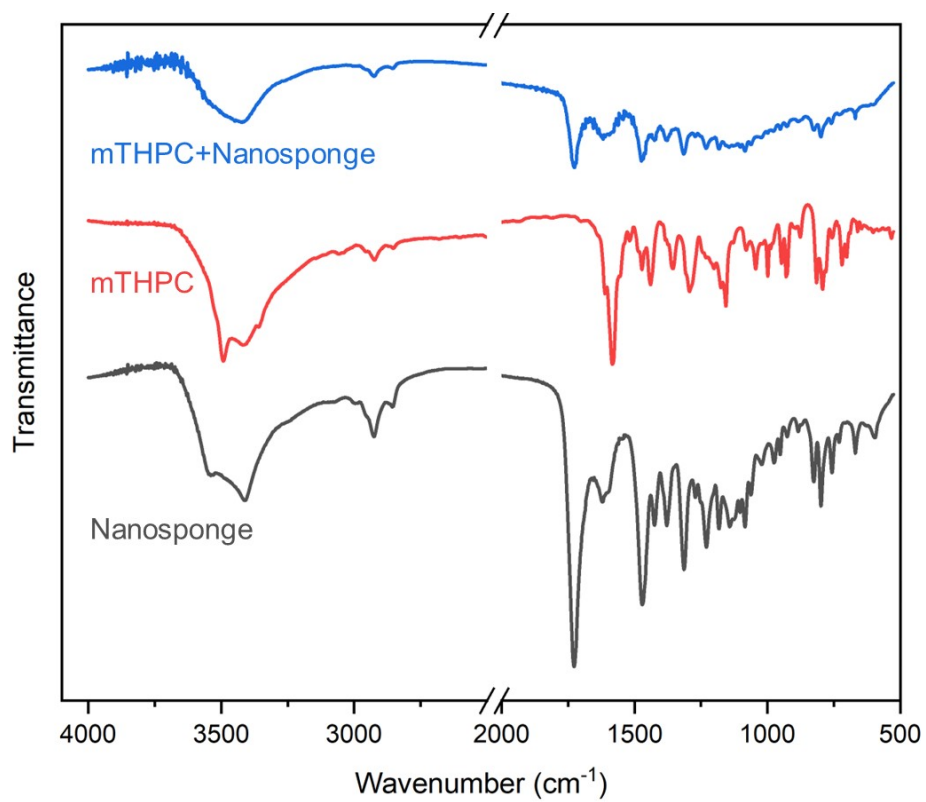


Fig. S4. Fourier transform infrared spectra of mTHPC, Nanosponge and mTHPC+Nanosponge.

Host-Guest Chemistry

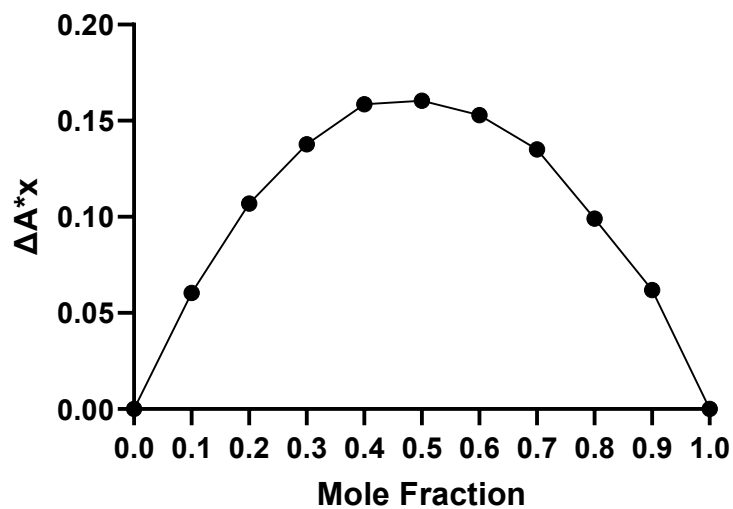


Fig. S5. Job plot ($[\text{CB}[n] \text{ 1}] + [\text{mTHPC}] = 10 \mu\text{M}$) of mole fraction of acyclic $\text{CB}[n] \text{ 1}$ versus $\Delta A^* \chi$ at pH 7.4 (PBS).

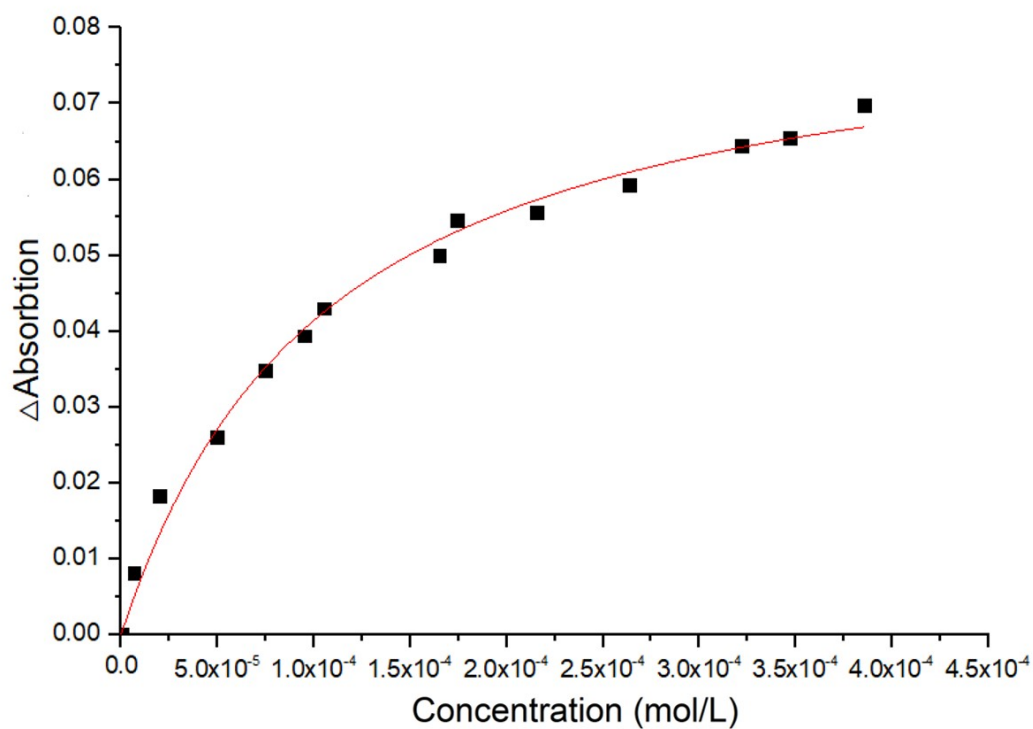


Fig. S6. Plot of the ΔAbs (A-A0) at 425 nm as a function of the concentration of acyclic $\text{CB}[n] \text{ 1}$. The solid line represents the best non-linear fitting of the data based on a 1:1 binding model ($K_a = (1.01 \pm 0.12) \times 10^4 \text{ M}^{-1}$).

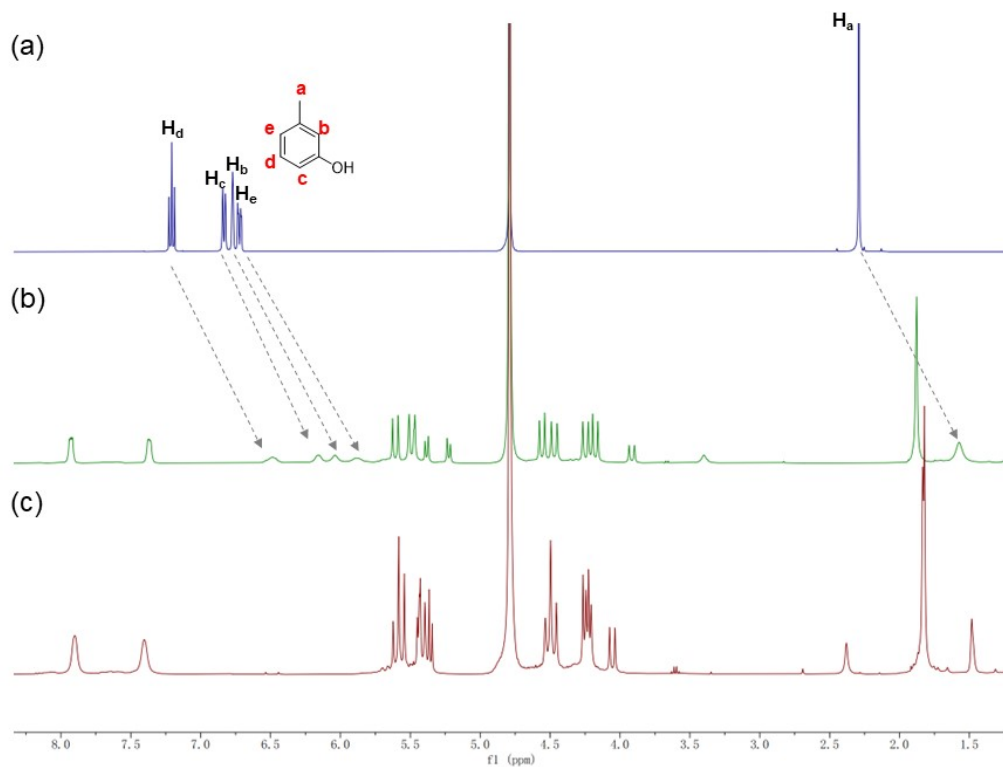


Fig. S7. ¹H NMR spectra recorded for (a) m-cresol (b) m-cresol and acyclic CB[n] 1 (c) acyclic CB[n] 1.

In Vitro Study

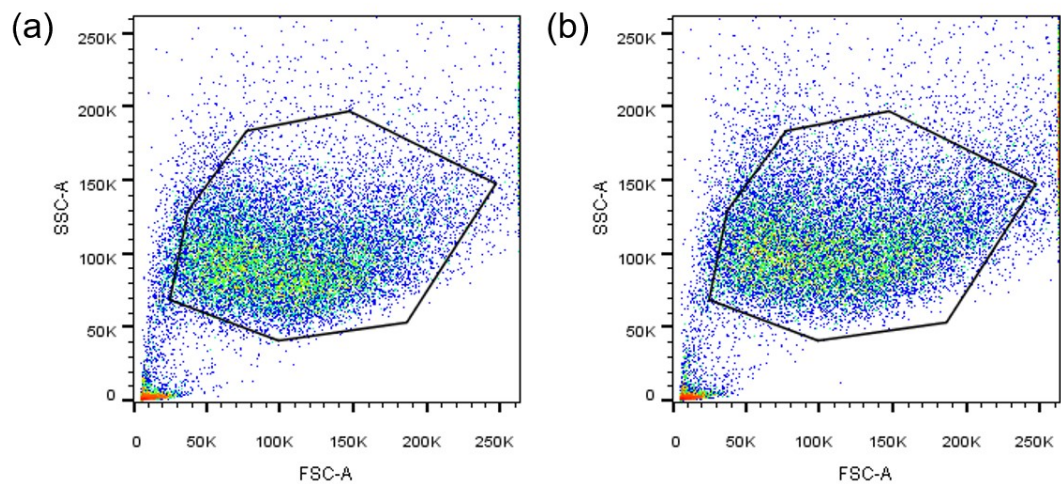


Fig. S8 Flow cytometry of HeLa cells treated with (a) mTHPC and (b) mTHPC-loaded nanosponges.

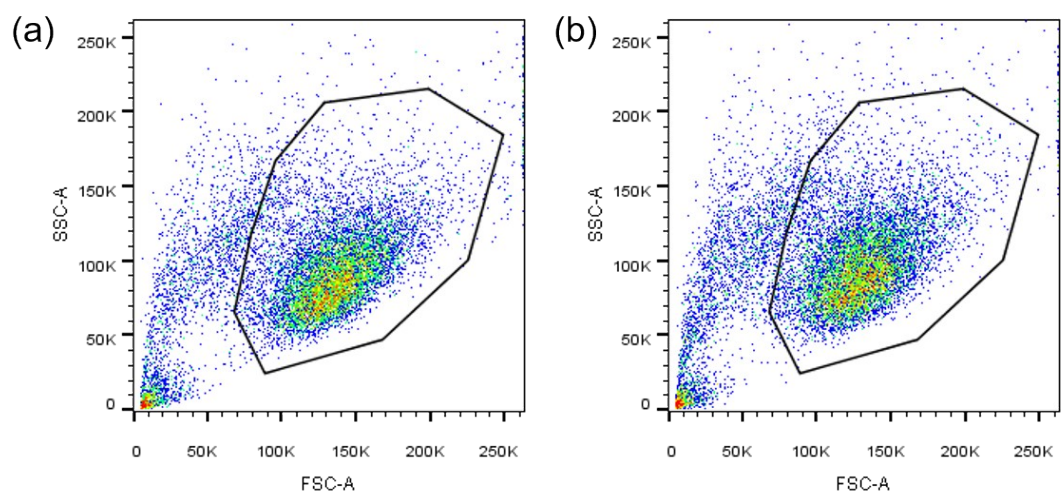


Fig. S9 Flow cytometry of B16-F10 cells treated with (a) mTHPC and (b) mTHPC-loaded nanosponges.

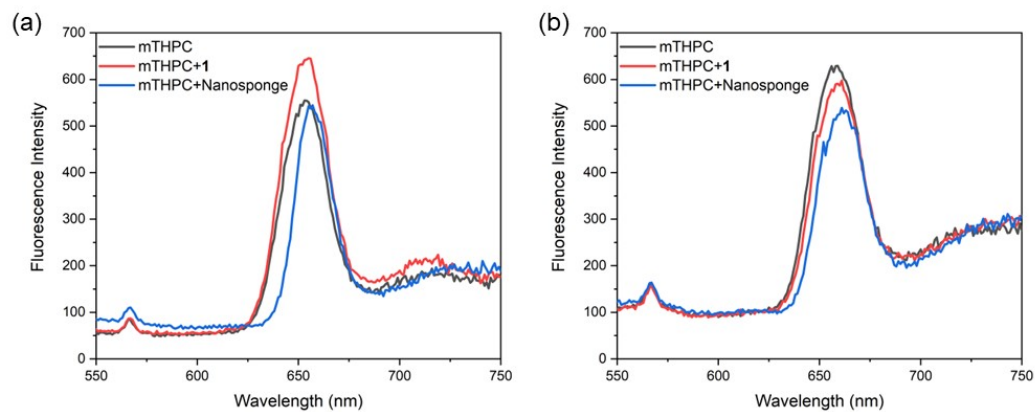


Fig. S10. (a) Fluorescence emission spectra of mTHPC, acyclic CB[n] **1** + mTHPC and mTHPC@nanosponge ($[mTHPC] = 2 \mu M$, $[1] = 15.6 \mu M$, $[Nanosponge] = 0.02 \text{ mg/mL}$, load ratio=6.8%). (b) Fluorescence emission spectra of mTHPC, acyclic CB[n] **1** + mTHPC and mTHPC@nanosponge ($[mTHPC] = 10 \mu M$, $[1] = 15.6 \mu M$, $[Nanosponge] = 0.02 \text{ mg/mL}$, load ratio=34%). Laser excitation : 405 nm.

In Vivo Study

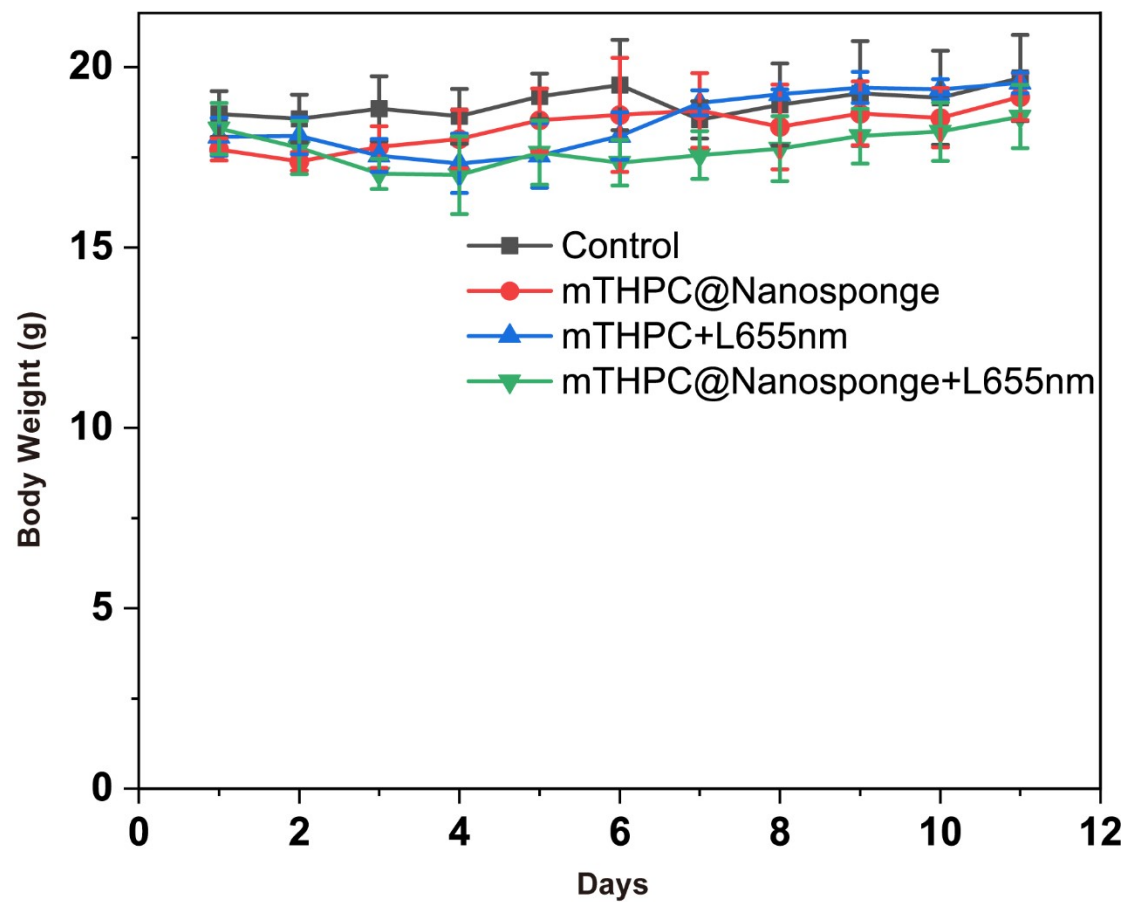


Fig. S11. The body weight variation of mice from each group.